

Atomic and Electronic Structures of GaN/ZnO Alloys

Shuzhi Wang* and Lin-Wang Wang

Computational Research Division, Lawrence Berkeley National Laboratory,
One Cyclotron Road, Mail Stop 50F, Berkeley, California 94720, USA

(Received 20 August 2009; published 10 February 2010)

A new model Hamiltonian is developed to describe the *ab initio* energy differences of the nonisovalent alloy configurations based on the semiconductor electron counting rule. Monte Carlo simulations using this Hamiltonian show strong short range order of the GaN/ZnO alloy, which has significant effects on its electronic structure. We also predict further reduction of the band gap by increasing the synthesis temperature.

DOI: 10.1103/PhysRevLett.104.065501

PACS numbers: 61.66.Dk, 71.20.Gj

Hydrogen generation via water photosplitting is a subject of recent interest due to concerns of global warming and fossil fuel consumption [1,2]. Metal oxides are attractive for this task due to their low toxicity, cheap manufacturing processes, and stability in aqueous solutions [1,3]. A recent breakthrough is the discovery of GaN/ZnO, a pseudobinary semiconductor alloy [4–7], which has a water splitting efficiency much higher than other oxides under visible light. This high efficiency is partly attributed to its band gap of 2.7 eV (with 13% ZnO), which is lower than the 3.5 and 3.4 eVs band gaps of GaN and ZnO [8,9].

The mechanism of this band gap lowering is currently under intense debate, with theories varying from *p-d* repulsion [10–12], to Zn impurity levels [11,13], to volume deformation and structural relaxation [10]. Compounding this problem is the uncertainty of the atomic structure of GaN/ZnO. While experimental TEM images and x-ray diffraction data show that the alloy is in a coherent wurtzite (WZ) crystal structure, it is not clear whether it forms a uniform alloy or shows clustering behaviors. GaN/ZnO represents a new class of alloys (denoted as III–V/II–VI), which is different from isovalent semiconductor alloys (e.g., III–V/III–V, II–VI/II–VI). One can characterize it as a locally nonstoichiometric alloy. Many people still believe a relatively uniform alloy of this type cannot be formed. In a way this system is like the codoping system, where one cation impurity (e.g., Zn) will be accompanied by one anion impurity (e.g., O), except that here the composition x is much larger. Previous theoretical calculations are based on completely random systems [10–12], completely ordered superlattice systems [12], or impurity systems [11]. They have also used small supercells (e.g., with 16, 32, or 108 atoms) which might not be able to describe the correct atomic structures.

In this Letter, we take a holistic approach. We first develop a model Hamiltonian describing the *ab initio* energies of different atomic configurations. This model Hamiltonian is then used in Monte Carlo (MC) simulations to study the atomic structures of systems containing over a thousand atoms. The equilibrium atomic structures from the MC simulations at different temperatures are then used

to calculate their electronic structures. We found that at the experimental synthesis temperature of 1100 K, uniform alloys can indeed be formed, albeit with strong short range order. Consequently, their electronic structure is very different from the completely random alloy. We also predict that a higher synthesis temperature can yield even lower band gaps.

There are traditional cluster expansion models to describe the energies of different alloy configurations [14]. However, here we will develop our model based on the chemically intuitive electron counting rule in semiconductors [15], which is also known as Pauling's electrostatic valence rule [16] in ionic systems. It states that each cation and anion have a fixed valence charge regardless of their local atomic environments. In our case, this can be Ga^{+3} , Zn^{+2} , N^{-3} , O^{-2} . To test this, we have analyzed the atomic charges based on density functional theory (DFT) calculations for different alloy configurations. Although the charges depend on the decomposition procedure, the standard deviation for the same type of atoms (regardless of their local bonding environments) is 30 times smaller than their absolute values. One good feature about our model is that it will not depend on the absolute ionic charges, as long as $Q(\text{Ga}) = -Q(\text{N})$, $Q(\text{Zn}) = -Q(\text{O})$, and $Q(\text{Ga})$, $Q(\text{Zn})$ are different, which are all found approximately true in our analysis.

We next assume Q_i is reached by the nearest-neighbor (j) charge flow, to be denoted as C_{ij} , where i and j are atom indices. In other words,

$$Q_i = \sum_{j \in \text{Ennb}} C_{ij}(\sigma). \quad (1)$$

Here σ denotes the atomic configuration in the system, where Ga, Zn occupy the WZ cation sites and N, O the anion sites. Note by definition $C_{ij} = -C_{ji}$, and $Q_i = Q(\text{Ga})$ if atom i is Ga, and so on. Now assuming that it costs energy to have a charge flow C_{ij} , we can define

$$J(\sigma) = \sum_{i=1}^N \sum_{j \in \text{Ennb}} C_{ij}^2(\sigma) \quad (2)$$

and use it as a measure of the total energy for this configura-

ration. Thus our model is

$$E_{\text{tot}}(\sigma; x) = a[J(\sigma; x) - J^*(x)] + E_{\text{tot}}^*(x). \quad (3)$$

Note $E_{\text{tot}}^*(x) = (1-x)E_{\text{GaN}} + xE_{\text{ZnO}}$ and $J^*(x) = (1-x)J_{\text{GaN}} + xJ_{\text{ZnO}}$. For a given σ , the $C_{ij}(\sigma)$ should be determined from the charge balance Eq. (1). But there are more $C_{ij}(\sigma)$ than Q_i in Eq. (1). We thus further require that the $C_{ij}(\sigma)$ which give the smallest J in Eq. (2) should be used. It can be proved that this is equivalent to requiring that $C_{ij}(\sigma)$ have no vorticity; i.e., the sum of $C_{ij}(\sigma)$ along any closed loop in the bond topology should be zero. This is further equivalent to $C_{ij}(\sigma) = V_j(\sigma) - V_i(\sigma)$, which is like a static electric field (with zero curl), that can be written as the gradient of an electric potential.

Now for a given configuration σ , the solution of $V_i(\sigma)$ will be a linear equation of dimension N , where N is the number of atoms in the system. It can be proved that if the relative values of $Q(\text{Ga})$ and $Q(\text{Zn})$ are changed, the $J(\sigma; x) - J^*(x)$ in Eq. (3) will only change a uniform prefactor for different σ . Thus, our model is independent of the $Q(\text{Ga})$ and $Q(\text{Zn})$. However, for simplicity, we will use $Q(\text{Ga}) = +3$ and $Q(\text{Zn}) = +2$ in the following.

Equation (3) is tested using direct *ab initio* DFT calculated energies for 91 random configurations of $2 \times 2 \times 2$ and $3 \times 3 \times 3$ supercells (containing 32 and 108 atoms, respectively) with ZnO compositions ranging from 0 to 1. The WZ lattice constant follows the Vegard's law $b(x) = (1-x)b_{\text{GaN}} + xb_{\text{ZnO}}$. The *ab initio* calculations are done with the Vienna *ab initio* simulation package (VASP 4.6.35) [17], with the 3d electrons of Ga and Zn treated as valence electrons.

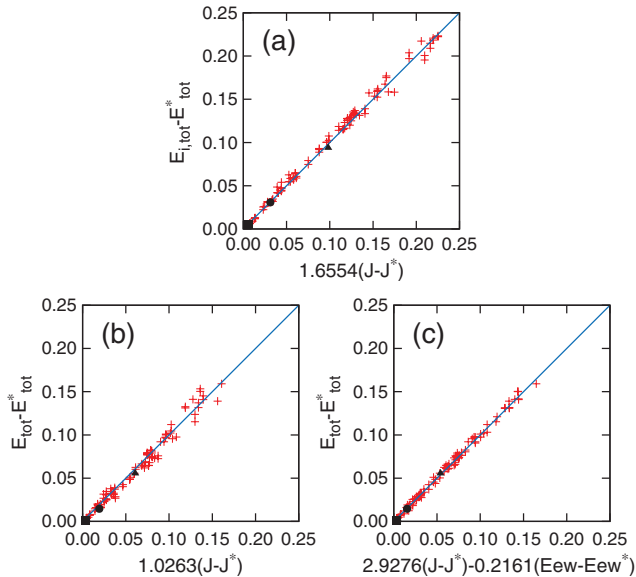


FIG. 1 (color). Energy comparison between our models and the DFT energies (in eV/atom) for unrelaxed case (a), relaxed case (b), and two parameter form (c). Red crosses: small supercell configurations. Black filled symbols: the random configuration (triangle) and MC snapshots at 300 K (square) and 1100 K (circle) of 1280-atom supercell. Blue lines: the exact curve.

In Fig. 1(a), our model Hamiltonian with a fitting parameter $a = 1.6554 \text{ eV}/e^2$ is tested with the DFT energies of alloys with ideal WZ atomic sites (without atomic relaxation). The fit is excellent with a standard deviation $s \sim 6 \text{ meV}/\text{atom}$ and correlation coefficient $\rho = 0.986$. The ideal lattice site situation corresponds to pure chemical bond (thus charge flow) energy, where we expect our model to work best. In Fig. 1(b), our model with a fitting parameter $a = 1.0263 \text{ eV}/e^2$ is compared with the *ab initio* energies of relaxed alloy configurations. The agreement is still good ($s \sim 7 \text{ meV}/\text{atom}$, $\rho = 0.973$), but less accurate than the unrelaxed ones. To further improve our model Hamiltonian for this case, we have included the Ewald energy $E_{\text{ew}}(\sigma; x)$ [evaluated with lattice constant $b(x)$ and unrelaxed atomic positions] using $Q(\text{Ga}) = +3$, $Q(\text{Zn}) = +2$, $Q(\text{N}) = -3$, $Q(\text{O}) = -2$. Furthermore, we define $E_{\text{ew}}^*(x) = (1-x)E_{\text{ew}}(\text{GaN}; x) + xE_{\text{ew}}(\text{ZnO}; x)$, where $E_{\text{ew}}(\text{GaN}; x)$ and $E_{\text{ew}}(\text{ZnO}; x)$ are Ewald energies of pure GaN and ZnO evaluated with lattice constant $b(x)$. Now we have

$$E_{\text{tot}}^{\text{relax}}(\sigma; x) = a'[J(\sigma; x) - J^*(x)] + b'[E_{\text{ew}}(\sigma; x) - E_{\text{ew}}^*(x)] + E_{\text{tot}}^*(x). \quad (4)$$

The comparison of this two parameter form model energy (with $a' = 2.9276 \text{ eV}/e^2$, $b' = -0.2161$) and the *ab initio* energy is given in Fig. 1(c) ($s \sim 3 \text{ meV}$, $\rho = 0.996$). The agreement is even better than the unrelaxed case. The above approaches have also been tested for AlN/ZnO alloys and a similar accuracy was found.

We next use our model Hamiltonian in MC simulations to study the atomic structures for their configurational degrees of freedom. Although Eq. (4) is more accurate than Eq. (3) for the relaxed energy, in our MC simulations test, we found that the resulting atomic structures are similar. Thus we have used Eq. (3) to speed up our MC

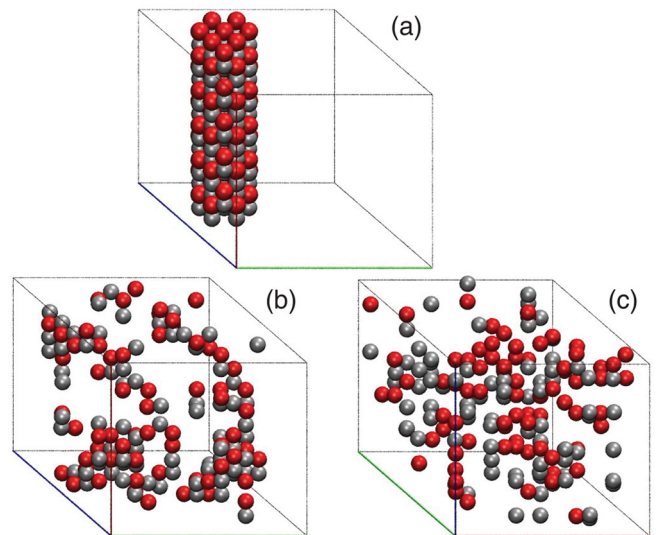


FIG. 2 (color). Snapshots of the 300 K (a) and 1100 K (b) MC simulation runs, and a randomly generated configuration (c). Zn: silver gray balls. O: red balls. Ga and N atoms are not shown.

simulations. MC simulations are done for $T = 1100$ K (the experimental synthesis temperature [6], which is much lower than the melting temperatures of ZnO and GaN) and 300 K with a $8 \times 8 \times 5$ WZ supercell, which has sides of length ~ 25 Å and contains 1280 atoms. The experimental ZnO composition of $x = 0.125$ is used. The lattice parameters of the supercell are fixed in the simulations according to Vegard's law. Two types of trial MC moves are used: (1) nearest-neighbor Zn-Ga, (and O-N) swapping; (2) Zn-O and Ga-N bonded pair swapping. A parallel tempering (PT) method [18] is used to speed up the simulation at 300 K. 1×10^8 MC steps were performed for both 1100 and 300 K MC simulations.

Snapshots of the 1100 and 300 K MC simulations together with a randomly generated configuration are shown in Fig. 2. Their Zn-O pair correlation functions are shown in Fig. 3 (the 1100 K correlation function is essentially unchanged when a much larger, $13 \times 13 \times 8$ supercell is used). From Fig. 2, we can see that at room temperature, the system is phase separated. However, at 1100 K, the alloy is relatively uniform, but with strong short range order as shown in Fig. 3. It is also difficult to characterize the structure as a codoping case because the Zn (also O) atoms are connected to each other.

We next study the electronic structures of these three cases shown in Fig. 2: the 300 and 1100 K snapshots, and the random configuration. Their atomic structures are relaxed with VASP. Their unrelaxed and relaxed total energies are shown in Figs. 1(a)–1(c), which fit nicely to the predicted energies, confirming once again the accuracy of our energy model. The relaxed systems are then calculated with the PETOT code [19] with norm-conserving pseudopotentials (the Zn and Ga $3d$ electrons are still included in the valence). The resulting LDA band gap of the 1100 K system is 1.4 eV. This small value is due to the LDA band gap error. The LDA calculated GaN and ZnO band gaps are 1.89 and 0.66 eVs, compared with the experimental values of 3.5 and 3.4 eVs, respectively. If these end point LDA band gaps are corrected while keeping the bowing parameter the same, we get a corrected theoretical band gap for the 1100 K system as: 3.15 eV. Although many theoretical studies in the literature have used this approach [12], the very different band gap corrections for GaN and ZnO are worrisome since it implies very different conduction band

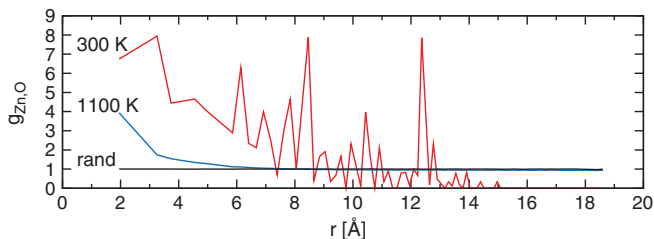


FIG. 3 (color). Zn-O pair correlation functions of the 300 K (red) MC, 1100 K (blue) MC, and randomly generated configurations (black).

alignment. To correct this, we have modified s , p , d non-local potentials to fit the bulk band gaps of ZnO and GaN, while keeping the valence band levels fixed. The modified nonlocal potentials are then used to calculate the electronic structures of the alloy systems. This approach has been successfully used to study nanostructures and other alloys [20–22]. We have tested a few sets of the fitting parameters, and they all yield very similar alloy results, confirming the reliability of this LDA+C (correction) procedure.

Using this LDA+C procedure, the calculated 1100 K alloy band gap is 3.04 eV, while the 300 K and random alloy results are 3.12 and 2.02 eVs, respectively. The calculated 1100 K alloy band gap seems to be 0.3 eV higher than the experimental result. However, there could be random fluctuations due to different configurations. To address that, we have calculated four additional configurations (snapshots during MC simulation) and found their band gaps being 2.958, 3.037, 2.960, 2.956 eVs. Thus the lowest gap is 0.08 eV lower than the value we discussed above. Most importantly, we notice that in their diffuse reflectance optical measurement, the band gaps for pure ZnO and GaN are 3.2 and 3.4 eVs [5,6], whereas we have used 3.4 and 3.5 eVs [8,9] in this work. Thus the experimental band gap lowering is 0.67 eV, which is quite close to our value of 0.53 eV.

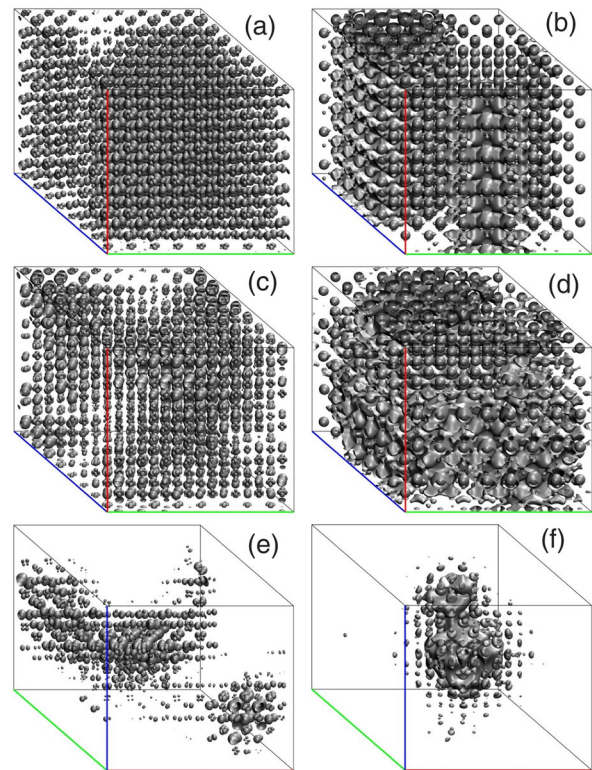


FIG. 4 (color online). VBM and CBM charge density isosurfaces of the 300 K MC snapshot (a) and (b), 1100 K MC snapshot (c) and (d), and the randomly generated configuration (e) and (f). The isosurfaces contain 80% of the electron or hole charges.

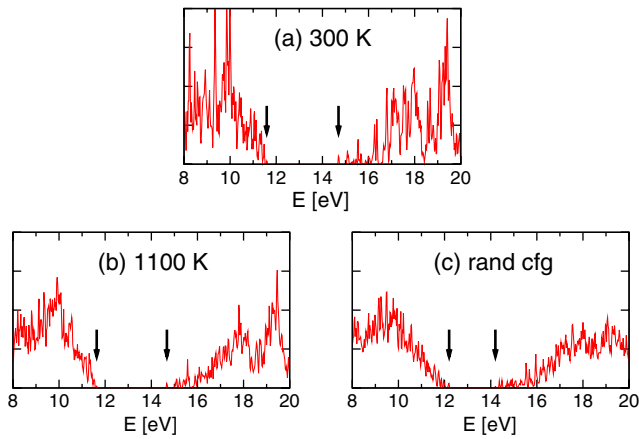


FIG. 5 (color online). Plots of the density of states of the 300 K MC snapshot (a), 1100 K MC snapshot (b), and the randomly generated configuration (c). y axis is in arbitrary unit. The vertical arrows indicate the CBM and VBM states.

Figure 4 shows the conduction band minimum (CBM) and valence band maximum (VBM) wave functions for the three cases calculated using the LDA+C procedure, and their density of states are plotted in Fig. 5. Based on wave function charge density projections on individual atoms, we found that, for the 300 K, the CBM charges on Zn and O atoms are similar, and they are 6 times larger than the Ga and N charges. On the other hand, for the random case, the CBM charge on Zn is very small, and the charge on O is 5 times larger than the charges on Ga and N. For 1100 K, the situation is more close to 300 K than to the random case. For VBM, the N has the largest wave function charge in all cases, although in the random case, the charge on Zn has a similar magnitude. Thus the random case is similar to the Zn acceptor and O donor impurity levels picture [11]. When these impurities are not compensated (no ordering), they form these localized impurity levels. However, in the 1100 K alloy system, the short range order removes these impurity like states, and changes the situation to a band alignment like picture. We also calculated the localization volume V_{loc} (defined as $1/\int \psi^4 d^3r$) of the band edge wave functions, and found that the random case has a much smaller localization volume in both VBM and CBM (119 and 171 \AA^3) than the 300 K and 1100 K cases (1071 and 2129 \AA^3 for 300 K, 706 and 2617 \AA^3 for 1100 K), thus corroborating Fig. 4.

Compared to the results of previous theoretical studies [10,12], the optical bowing parameter (4.8) estimated from our calculated 1100 K alloy band gap is quite close to that in Ref. [10] (4.05), which also agrees well with experiment [6] (~ 6 as estimated from their data), but is much smaller than that in Ref. [12] (11.5). Our calculation shows that ordering plays an important role which increases the band gap and reduces the bowing parameter. We further predict a higher synthesis temperature will lead to smaller band gaps. Our 1500 K calculation (following the same procedure) yields a band gap of 2.86 eV, 0.1 eV lower than the 1100 K results.

In conclusion, we found that at the experimental synthesis temperature, a uniform GaN/ZnO alloy can be formed, but with strong short range order. As a result, the band gap reduction is not due to the Zn acceptor and O donor levels. Instead, it is more like a GaN/ZnO type-II band alignment picture where CBM is close to Zn, and VBM is close to N, although there is no phase separation. The delocalized wave functions in this case can lead to high mobility, thus contributing to the high water splitting efficiency. We believe the experimentally synthesized sample is cooled and frozen at its high temperature configuration. The equilibrium room temperature structure is phase separating. We predict that, with even higher synthesis temperature, the band gap will be further reduced. Our model Hamiltonian provides a general approach to study this new type of locally nonstoichiometric alloys. Our preliminary tests show that it is applicable to many other locally nonstoichiometric systems.

This work was performed in the Helios Solar Energy Research Center which is supported by the Director, Office of Science, Office of Basic Energy Sciences, Materials Science and Engineering Division, of the U.S. Department of Energy under Contract No. DE-AC02-05CH11231. This research used the computational resources of the National Energy Research Scientific Computing Center (NERSC) and the National Center for Computational Sciences (NCCS).

*swang2@lbl.gov

- [1] T. Bak *et al.*, Int. J. Hydrogen Energy **27**, 991 (2002).
- [2] N. S. Lewis, MRS Bull. **32**, 808 (2007).
- [3] K. Rajeshwar, J. Appl. Electrochem. **37**, 765 (2007).
- [4] K. Sayama *et al.*, Chem. Commun. (Cambridge) **23** (2001) 2416.
- [5] K. Maeda *et al.*, J. Am. Chem. Soc. **127**, 8286 (2005).
- [6] K. Maeda *et al.*, J. Phys. Chem. B **109**, 20504 (2005).
- [7] K. Maeda *et al.*, Nature (London) **440**, 295 (2006).
- [8] B. Monemar, Phys. Rev. B **10**, 676 (1974).
- [9] *Semiconductors, II-VI and I-VII Compounds: Semimagnetic Compounds*, edited by U. Rössler, Landolt-Börnstein, New Series, Group III Vol. 41B (Springer, Heidelberg, 1999).
- [10] L. L. Jensen *et al.*, J. Phys. Chem. C **112**, 3439 (2008).
- [11] W. Wei *et al.*, J. Phys. Chem. C **112**, 15915 (2008).
- [12] M. N. Huda *et al.*, Phys. Rev. B **78**, 195204 (2008).
- [13] T. Hirai *et al.*, J. Phys. Chem. C **111**, 18853 (2007).
- [14] D. B. Laks *et al.*, Phys. Rev. B **46**, 12587 (1992).
- [15] M. D. Pashley, Phys. Rev. B **40**, 10481 (1989).
- [16] L. Pauling, *The Nature of the Chemical Bond* (Cornell University Press, Ithaca, NY, 1960), 3rd ed.
- [17] G. Kresse *et al.*, Comput. Mater. Sci. **6**, 15 (1996).
- [18] U. H. E. Hansmann, Chem. Phys. Lett. **281**, 140 (1997).
- [19] <http://hpcrd.lbl.gov/~linwang/PEtot/PEtot.html>.
- [20] J. Li and L.-W. Wang, Phys. Rev. B **72**, 125325 (2005).
- [21] J. Li and S.-H. Wei, Phys. Rev. B **73**, 041201(R) (2006).
- [22] J. Schrier *et al.*, Nano Lett. **7**, 2377 (2007).